INL/JOU-22-67783-Revision-0

Annealing influence on the microstructure of irradiated U-Mo monolithic fuel foils

June 2023

Fidelma Giulia Di Lemma, Jan-Fong Jue, Tammy L Trowbridge, Charlyne A Smith, Brandon D Miller, Dennis D Keiser Jr, Jeffrey Giglio, James I Cole

Changing the World's Energy Future

INL is a U.S. Department of Energy National Laboratory operated by Battelle Energy Alliance, LLC

DISCLAIMER

This information was prepared as an account of work sponsored by an agency of the U.S. Government. Neither the U.S. Government nor any agency thereof, nor any of their employees, makes any warranty, expressed or implied, or assumes any legal liability or responsibility for the accuracy, completeness, or usefulness, of any information, apparatus, product, or process disclosed, or represents that its use would not infringe privately owned rights. References herein to any specific commercial product, process, or service by trade name, trade mark, manufacturer, or otherwise, does not necessarily constitute or imply its endorsement, recommendation, or favoring by the U.S. Government or any agency thereof. The views and opinions of authors expressed herein do not necessarily state or reflect those of the U.S. Government or any agency thereof.

INL/JOU-22-67783-Revision-0

Annealing influence on the microstructure of irradiated U-Mo monolithic fuel foils

Fidelma Giulia Di Lemma, Jan-Fong Jue, Tammy L Trowbridge, Charlyne A Smith, Brandon D Miller, Dennis D Keiser Jr, Jeffrey Giglio, James I Cole

June 2023

Idaho National Laboratory
Idaho Falls, Idaho 83415

http://www.inl.gov

Prepared for the
U.S. Department of Energy
Under DOE Idaho Operations Office
Contract DE-AC07-05ID14517

Nuclear Materials and Energy 35 (2023) 101436

Contents lists available at ScienceDirect

Nuclear Materials and Energy

journal homepage: www.elsevier.com/locate/nme

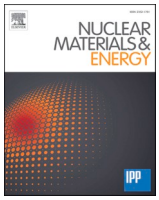

Annealing influence on the microstructure of irradiated U-Mo monolithic fuel foils

F.G. Di Lemma [a,1,*], J.F. Jue [a], T.L. Trowbridge [a], C.A. Smith [b,1], B.D. Miller [a], D.D. Keiser [a], J. J. Giglio [a], J.I. Cole [a]

[a] Idaho National Laboratory, P.O. Box 1625 MS 6000, Idaho Falls, ID 83415-6000, USA
[b] Glenn T. Seaborg Institute, Idaho National Laboratory, Idaho Falls, ID 83415, USA

ARTICLE INFO

Keywords:
U-10Mo
Monolithic fuel
Annealing
Irradiation
Decomposition

ABSTRACT

In this study we compared the microstructure evolution of U-Mo fuel foils produced with and without heat treatment at low burn-up via advanced post-irradiation examination. The aim of this study is to observe after irradiation the ways in which the fabrication processes have influenced fuel behavior at early-stage irradiation, as for very low burn up microstructural studies are lacking. In this work it was observed that the larger grain size detected in the heat-treated samples before irradiation led to decreased grain refinement after irradiation. Grain refinement was associated with the presence of small nano-size bubbles and precipitates. This phenomenon is hypothesized to influence early fuel swelling during reactor irradiation. Grain refinement was also observed to increase in regions where γ-U decomposition was present. Thus, it was enhanced in the samples fabricated without heat treatment. The heat treatment also increased the thickness of the U-Mo/Zr interface, namely of the UZr_2 layer. However, the influence of this layer on fuel performance needs further investigation. On one side, it may contribute to better mechanical bonding; on the other, it may influence swelling and blistering in the interaction layer as porosity increases when this layer is increased. This was observed especially in the presence of increased area containing low Mo concentration, and thus containing a higher fraction of the α-U phase, which is highly susceptible to irradiation induced swelling. Strong evidence of reverse transformation under irradiation (α-U + γ′-U_2Mo → bcc γ-U) was observed in these samples. While the precipitates (carbides and oxide) seem to be unaffected by the irradiation at these low burnups. However, further analyses are necessary at higher burn-up to assess the exact impact different heat treatments have on fuel performance.

Introduction

U-10 wt% Mo (U-10Mo) monolithic fuel is proposed, although not yet qualified, as a main candidate to convert some of the high power research reactors to low-enriched uranium fuels (LEU) [1,2,3]. U-10Mo is particularly interesting as it enables the continuation of current high-power performance while achieving the goal of increased proliferation resistance by reducing the enrichment of research reactor fuels. This fuel system has been extensively studied, including a long history of irradiation testing. Studies have demonstrated that U-Mo fuel can achieve very high burnup, while maintaining a stable microstructure and predictable swelling rates [1,4]. This paper focuses on the microstructure of the fuel after irradiation analyzing the effect of varying heat treatments on the early irradiation stage. Indeed, evaluating the microstructural changes during irradiation can permit to optimize fuel performance and can be used to establish the best fuel fabrication process. The microstructure of fuel is of main importance because it influences the physical and thermal properties of fuel [5]. Tailoring the initial microstructure of the fuel has been recently shown to also influence fission-induced recrystallization [6,7], which in turn may be used to control fission gas diffusivity [7,8]. Another parameter of relevance to be controlled during fabrication is Mo banding [9–16], as Mo variation in the fuel core can lead to gamma phase (γ-U) decomposition. This decomposition (bcc γ → α-U + γ′-U_2Mo) is undesirable because the γ-U phase, rather than the α-U (orthorhombic), in his bcc isotropic crystal structure provides swelling and oxidation resistance under irradiation [17].

* Corresponding author at: Characterization and Advanced PIE Division, Material Fuel Complex, Idaho National Laboratory, P.O. Box 1625 MS 6000, Idaho Falls, ID 83415-6000 USA.
E-mail address: FidelmaGiulia.DiLemma@inl.gov (F.G. Di Lemma).
[1] Glenn T. Seaborg Institute, Idaho National Laboratory, Idaho Falls, ID 83415, U.S.A.

https://doi.org/10.1016/j.nme.2023.101436
Received 18 July 2022; Received in revised form 2 March 2023; Accepted 21 April 2023
Available online 26 April 2023
2352-1791/© 2023 Published by Elsevier Ltd. This is an open access article under the CC BY-NC-ND license (http://creativecommons.org/licenses/by-nc-nd/4.0/).

Table 1
Details on sample fabrication and irradiation for the specimens analyzed.

Specimen	Unirr-B	Unirr-C	Irr-B	Irr-C
Alloying method	Arc melted	Vacuum casted	Arc melted	Vacuum casted
Homogenization	No	Yes	No	Yes
Post-cold-rolling annealing	No	Yes	No	Yes
Burn up (f/cm^3)	N/A	N/A	0.97×10^{21}	0.83×10^{21}
BOL[1] power average (kW/cm^3)	N/A	N/A	5.07	6.05
BOL power peak (kW/cm^3)	N/A	N/A	6.4	7.21

[1] BOL begging of life.

Recent papers [17–18] evaluate the effect of heat treatment processes on the microstructure of fuel before irradiation. While ref. [17] focused on monitoring the microstructure of the U-Mo fuel core under various annealing conditions with progressing longer times. In ref. [18] only one heat treatment process was analyzed. This heat treatment was chosen as prototypical of real reactor tested fuel plates. However, multiple parameters were analyzed not only fuel core grain structure and composition. In this study [17] molybdenum homogenization was observed, as an increase in grain size after the heat treatment. Other changes anlayzed included minimization of gamma phase decomposition in the fuel core and an increase in the interaction layer of the U-Mo fuel core with the Zr interlayer diffusion barrier. Finally, minimization of texture was observed in the U-Mo fuel core after the heat treatment. These were the desired effects of the heat-treatment which attempted to increase chemical homogeneity in the fuel core (e.g., reducing chemical banding and γ-U phase decomposition), to improve the U-Mo/Zr bonding, and to eliminate texture. Such microstructural changes are expected to improve irradiation fuel performance and enhance consistency. The aim of this study is to observe post-irradiation how these initial differences in microstructure generated by the fabrication process have influenced fuel performance. This work focuses novelty on the early stage of irradiation rather than high-burn up microstructural evolution, for which previous studies have been performed [4]. Comparison between the microstructure of irradiated and unirradiated fuel foils is described to identify possible microstructural features related to the pre-irradiation heat treatment that could impact fuel performance.

Advanced characterization techniques have been applied in these studies, namely scanning electron microscopy (SEM) with energy dispersive X-ray spectroscopy (EDS) and electron backscattered diffraction (EBSD). Traditional post irradiation examination (PIE) [19] do not permit direct chemical evaluation of the phases present in the fuel core. This analysis is of importance to detect the presence of γ-phase or its decomposition in the fuel core. Further an advanced sample preparation technique is presented in this study; the technique is large area lift-outs (LALO) using focus ion beam (FIB). This was applied to prepare mechanical-damage free specimens which are critical to the analyses of submicron microstructural features.

Experimental procedure

Sample preparation

Samples analyzed in this study were obtained from unirradiated and irradiated monolithic U-10Mo fuel plates. Four monolithic specimens used in this study contained foil that underwent different heat treatments as seen in Table 1. The various treatments are described in detail in the Refs. [18,20–22]. The U–10Mo alloys were cast by arc-melting (Unirr-B and Irr-B) or vacuum casting (Unirr-C and Irr-C). The ingots were laminated, in a carbon steel can, with a Zr foil on each surface. Such foil is added to act as a diffusion barrier in between the Al cladding and the fuel core, as this interaction has been proved detrimental during irradiation. The assembly was then preheated to 650 °C and hot-rolled. Typically, 20–40 rolling passes were required to reach the final desired foil thickness. The total time exposure during hot rolling to 650 °C was estimated at approximately 300 min. Further cold-rolling step was performed to obtain targeted foil thicknesses, followed by hot isostatic press (HIP) bonding at 560 °C for 90 min at 100 MPa, with a heating and cooling rate of 280 °C per hour. The C series samples additionally underwent homogenization after casting, similar to that described in ref. [16], with an annealing temperature up to 1000 °C and an annealing time up to 7 days. These specimens (C series) were also annealed after the cold-rolling step to release stresses, similarly to the process described in ref. [22] (with temperatures up to 700 °C and an annealing time of up to 1 h). The B series samples were produced at laboratory scale, while the C series is using a vendor plate fabrication method. The irradiated specimens came from the mentioned unirradiated fuel plates series (B and C). The chosen samples had similar power density and burn-up (see Table 1) to evaluate the effect of heat treatment on fuel performance, without other confounding variables. Irradiation was performed in the advanced test reactor (ATR) at Idaho National Laboratory (INL) at low power. Detailed on irradiation are presented in Table 1.

These samples were following prepared for SEM analysis by cutting at the mid-plane. Following conventional mechanical polishing, the samples were deployed as described in detail in reference [4]. This method applied an auto-polisher with progressive finer polishing paper (from 9 μm to 1 μm) and a final mechanical polishing with colloidal silica (0.05 μm) to eliminate any residual mechanical stress introduced by sample preparation applied when EBSD analysis was performed. For a better surface finishing, and to observe nanometric features in the irradiated samples, a FIB lift out technique and glazing surface polishing by focus ion beam was performed, similar to the procedure in Ref. [23] and described in the following. A FEI Helios NanoLab plasma focused ion beam and scanning electron microscope (PFIB/SEM) was utilized to prepare large area lift outs (LALOs) for microstructural characterization analysis. Unlike the conventional TEM lamellae [24–25], the LALOs are larger in volume and surface area to conveniently perform chemical composition and crystallographic analyses, also minimizing radiation fields during the SEM analyses. Furthermore, LALOs offer the advantage of large fuel cross-section examination by eliminating oxidation layers and other artifacts that may be present on the polished surface of the fuel specimen, which permit to obtain high resolution information on nanometric features. In this work a voltage and current of 30 kV and 1.6nA, respectively was used. First protective platinum layers of 50 μm × 4 μm × 3 μm are deposited on the regions of interest (ROIs) for LALO extraction at 12 kV and 4.5nA. Extraction of the ROIs is obtained by coarse trenching similarly to demonstrations in Refs. [24–25]. Once extracted the LALOs are mounted on a molybdenum grid via Pt deposition. Iteratively thinning was performed on one face at 30 kV and low beam currents with the final FIB polish performed at 6.7nA to minimize xenon beam ion damage.

Instruments and data collection

The SEM/EDS data were collected using a JEOL-7000 and a JEOL-IT-500-HR, each equipped with an Oxford EDS X-max 50 and Ultimax-65 respectively, for elemental analysis. Analyses were conducted at 20 keV. The current was optimized to obtain a deadtime (DT) below 50 %. X-ray maps were collected with a dwell time of 100 ms for a total of at least 10 frames and with a resolution of 512 × 384 pixels. EDS analyses were conducted via the standardless method. The described detector is calibrated yearly for reliable measurements. Images were collected in secondary-electron (SE) mode for morphological information and in backscattered-electron (BSE) mode for compositional information.

The analyses via EBSD were conducted using the JEOL-IT-500-HR equipped with an Oxford symmetry detector (1.2 megapixel, 3000 pps). Parameters employed in data collection are reported in reference

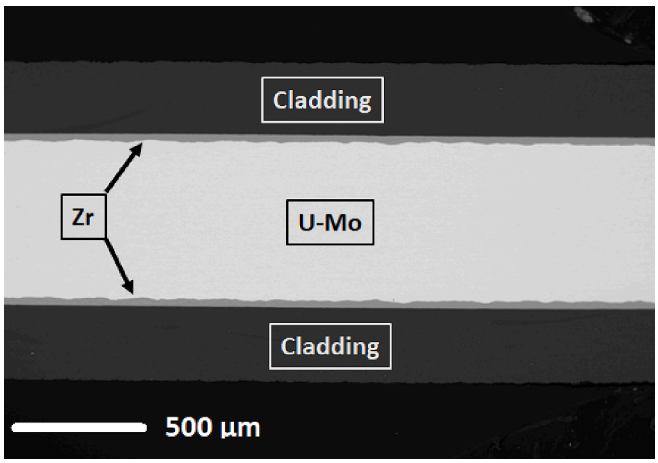

Fig. 1. Example of a typical monolithic plate fuel cross section before irradiation, showing the major features at low magnification such as the U-Mo fuel core, the Zr interlayer, and the Al cladding.

[18]. All EBSD measurements were performed with the sample tilted at 70°toward the EBSD detector. Patterns were indexed with a user-defined crystal structure for U-Mo BCC space group 229 Im3m (a = b = c = 3.44). EBSD data were collected with Aztec 5.1. The cleanup routine included wild-peak removal and corrected the zero solution via an iterative neighboring correlation with at least six neighboring grains. EBSD data collected were analyzed and elaborated with CHANNEL 5 and Atzec Crystal.

Results

Grain structure and gamma phase decomposition

An example of a typical monolithic fuel plate, obtained by SEM, is shown in Fig. 1, in which the fuel core, cladding, and interlayer are highlighted. The microstructure of the fuel core before irradiation is shown in Fig. 2 and Fig. 3 by high magnification SEM images and EBSD. These images reveal typical features of the samples, such as γ-phase decomposition and grain size. Unirr-B sample (Fig. 2), which did not receive the heat treatment process, as previously described in reference [18], showed elongated grains and high areas of γ-phase decomposition. It is clear from Fig. 3 that after the heat treatment (as performed in Unirr-C) the grain structure is modified. The specimen presents larger grains, which are equiaxed. Moreover, the decomposition regions are minimal in this sample and are mostly associated with the presence of grain boundaries.

After irradiation (Fig. 4 and Fig. 5) the analyses showed that γ-phase decomposition is no longer visible in both samples. Wavy U-Mo grain boundaries are formed with nano-size pores associated with their grain boundaries. These features were present in both samples, regardless of the heat treatment process. Previous work by Di Lemma et al. [4] showed that at very high burnup (i.e., $>6 \times 10^{21}$ f/cm^3), much higher than the one analyzed in this study (less than1 $\times 10^{21}$ f/cm^3), the pre-irradiation gamma phase, uranium grain boundaries can no longer be identified, as these regions have completed the grain refinement (e.g., polygonization process). Indeed, in previous studies [26–27] grain refinement was observed at 2.5-3 $\times 10^{21}$ f/cm^3 starting at the grain boundary. With increasing burn-up the refinement front will move towards the center of the grains. Thus, eliminating the original grain

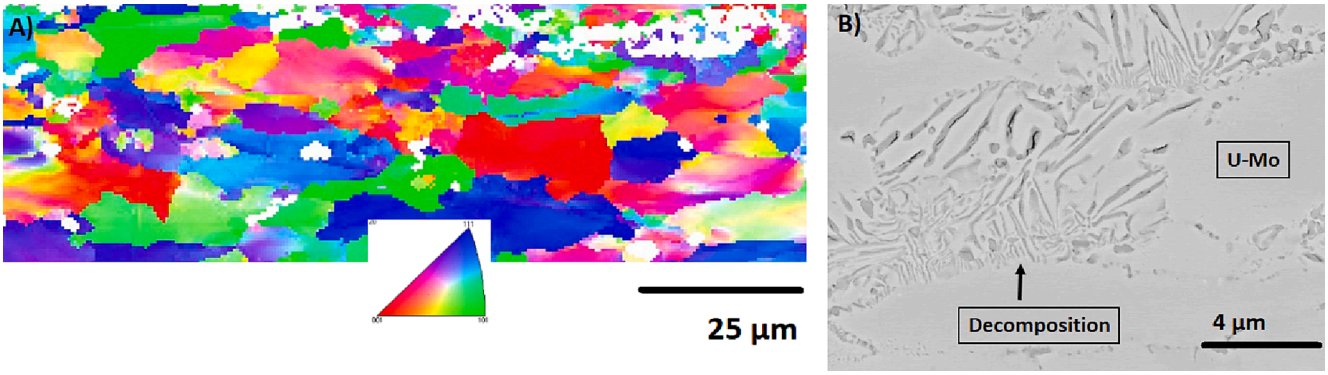

Fig. 2. Grain structure for Unirr-B. A) EBSD inverse pole figure showing the grain size and orientation. White pixels are unindexed areas associated with γ-phase decomposition. B) High magnification BSE image showing large γ-phase decomposition regions.

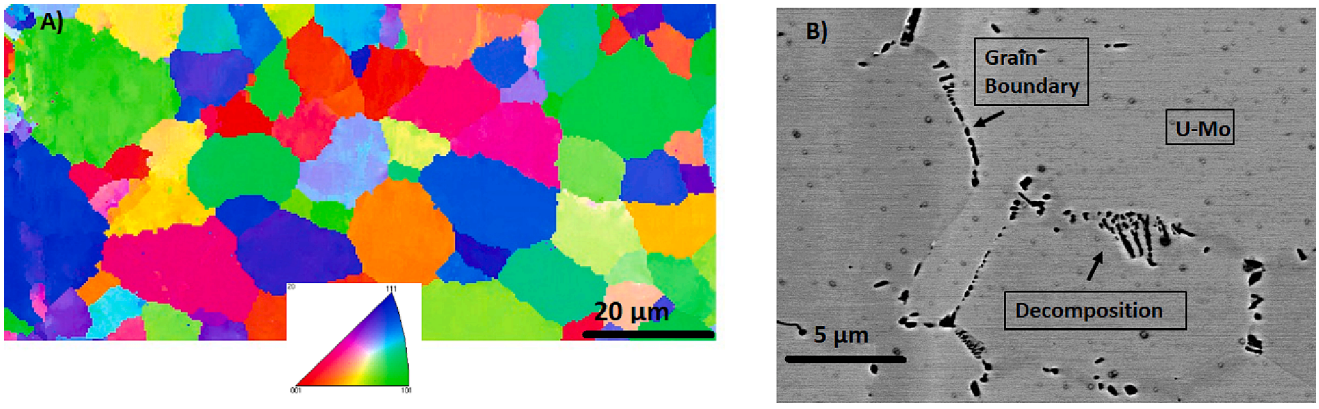

Fig. 3. Grain size for Unirr-C sample. A) EBSD inverse pole figure showing the grain size and orientation. B) BSE image at high contrast showing minimal γ-phase decomposition on the grain boundaries.

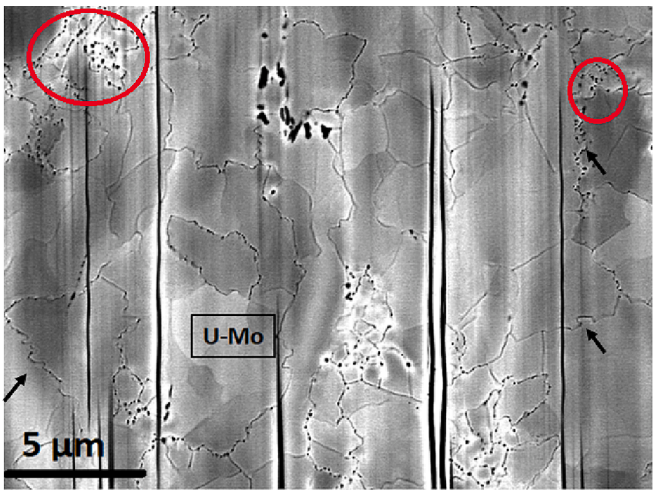

Fig. 4. High contrast BSE image for sample Irr-B, showing grain structure and porosity at grain boundaries of small grains after irradiation. The vertical dark lines are generated by sample preparation artifact during FIB preparation. Examples of wavy grain boundaries have been highlighted with arrows. While nanopores are highlighted with red circles. (For interpretation of the references to color in this figure legend, the reader is referred to the web version of this article.)

structure and grain boundaries. However, some pre-irradiation texture in the high burnup samples without treatment was observed to still exist [4]. In this study, Fig. 4 shows that also at these lower burn-up rates grain restructuring starts to develop at the grain boundaries, but most of the original grains and boundaries are maintained.

Zr layer and its interaction with the U-Mo fuel core

The Zr diffusion layer barrier seems to not be affected by the irradiation at the investigated low burn-up, as seen in Fig. 6, with the material presenting large grain size (around 20 µm) even after irradiation regardless of the heat treatment. Similar grain structures were observed in previous analyses for both unirradiated and irradiated U-Mo monolithic samples [26]. Moreover, the typical features of the U-Mo/Zr interaction layer are observed in the samples before irradiation (Fig. 7), regardless of the heat treatment, as described in detail in reference [18]. These are in line with historic data [1], describing this layer to be composed of the UZr_2 layer, a low Mo region related to the presence of α-U and Mo_2Zr phases. No significant differences at the U-Mo/Zr interface were observed before irradiation for the samples with different heat treatment (Unirr-B vs. Unirr-C), except a slightly larger average UZr_2 sublayer thickness in the fuel plate that underwent heat treatment (Unirr-C). After irradiation in Fig. 8, tiny fission gases bubbles have been observed in the low molybdenum region of the interaction layer. The formation of these bubbles may be related to the presence of α-U developed in the low Mo region, as this phase has been demonstrated to be more susceptible to fission gases bubble. While the γ-phase has been demonstrated to retain fission gases to higher burn up thanks to the precipitation of gases in nano-sized superlattice bubbles [1]. Similar bubble formation in low Mo regions was observed in ref. [20] (at burn ups $> 2.5 \times 10^{21}$ f/cm^3). It is possible that phase reversion will occur at higher burn-ups, as hypothesized in ref. [20], but further studies are necessary.

Precipitates (Carbides and Oxides)

From the analyses of the unirradiated sample, it was observed that more carbide and oxide precipitates were found in the fuel plate with heat treatment (Unirr-C). Analyses showed these to be over 1 % in volume fraction for the C series samples compared to under 0.5 % for the B series. Most of these precipitates seem to be aligned to form stringers. The precipitates were found to have larger dimensions in the non-heat-treated samples. An example of these precipitates is shown in Fig. 9. The reason for this may not be related to the heat treatment itself, rather it may be related to the initial uranium feedstock or from the fuel plate fabrication process. The precipitates influence on grain evolution during heat treatment was not evaluated in this study, as the work was focused on irradiation effect after fabrication. However, after irradiation the carbide and oxide precipitates are still present. Moreover, the heat treatment does not seem to impact carbide and oxide behavior even after irradiation as shown in Fig. 10. Most of the U-Mo and carbides and oxides interfaces are free from bubbles or precipitates at this burnup regardless of the heat treatment. However, such bubbles were observed in previous work at higher burn ups [29]. This phenomenon, although it generates fission gases bubbles which can affect swelling rates, has not been observed to influence fuel performance because their contribution is not substantial compared to the bubbles formed in the fuel core [30].

Mo distribution

SEM images seen in Fig. 11-A show significant Mo-banding in the sample without heat treatment (Unirr-B, A) before irradiation. While no visible Mo-banding before irradiation was observed in the sample with heat treatment, shown in Fig. 11-B. This is in line with formation mechanism's relation to insufficient homogenization during the alloying process [31]. A previous publication [18] shows these bands to be in the range 16 µm for the Unirr-B sample. Associated to chemical bands with

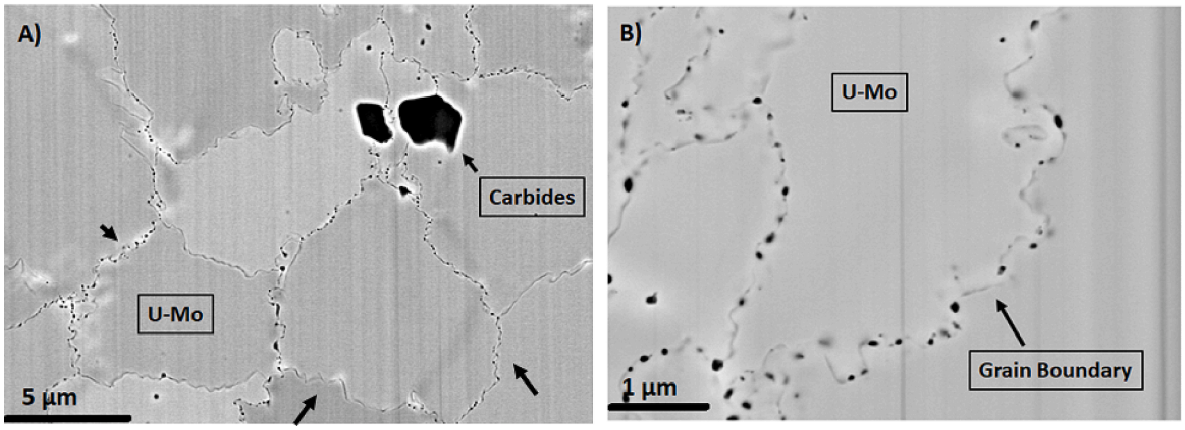

Fig. 5. High contrast BSE image for sample Irr-C, showing grain structure. In image A) carbides can be detected in the image and the larger grain are depicted. Wavy grain boundaries are highlighted by arrows. In image B) the high magnification image highlights the porosity formed at the grain boundaries.

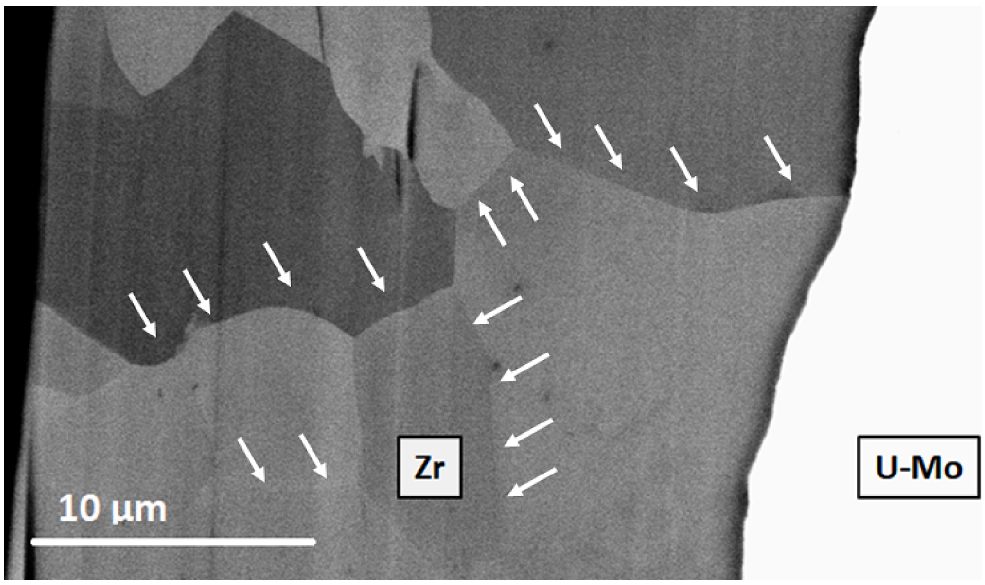

Fig. 6. SEM image of the Zr layer showing the big grains. Example is shown for the Irr-B, where some grain boundaries have been highlighted by arrow.

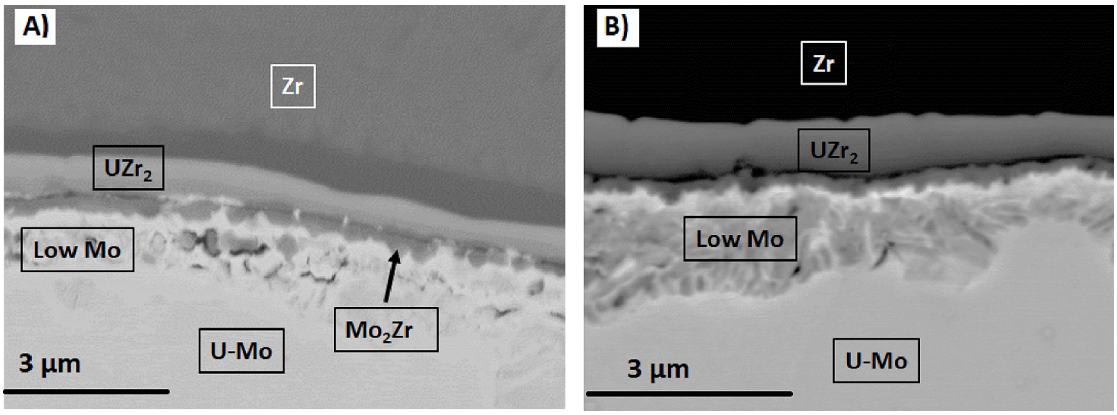

Fig. 7. Example images of the UMo/Zr interface. Highlighted with rectangles different chemical regions in the layer. A) Sample Unirr-B, B) Sample Unirr-C.

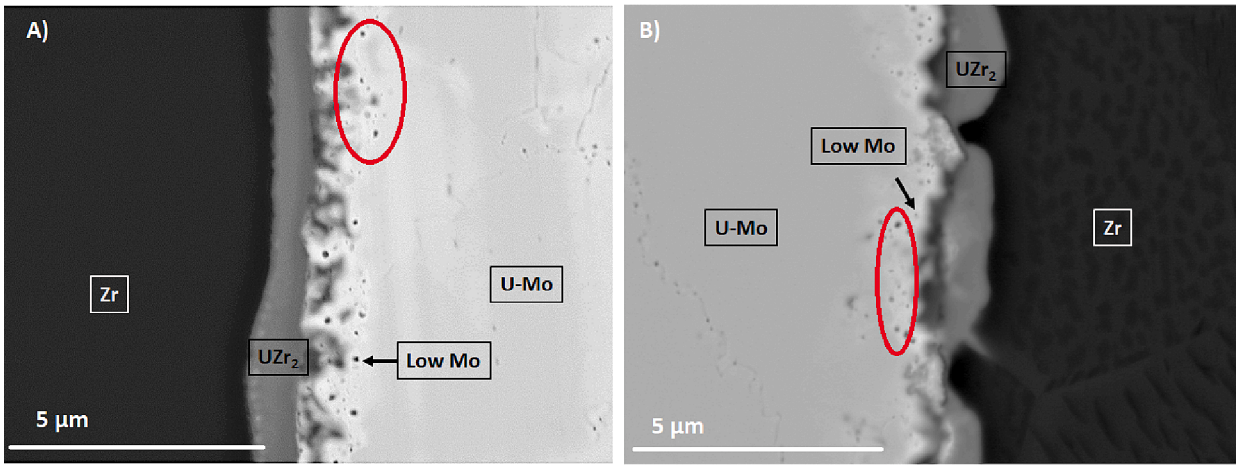

Fig. 8. Example of interaction layer after irradiation A) Irr-B, B) Irr-C. Both samples show the presence of porosities (highlighted by the red ellipses) in the low Mo region. (For interpretation of the references to color in this figure legend, the reader is referred to the web version of this article.)

low Mo concentration (bright color in Fig. 11-A) large and numerous decomposition areas were observed (around 19 % volume fraction for Unirr-B vs. 2 % for Unirr-C). These bands were still present in the irradiated fuel plate without heat treatment (Irr-B), as seen in Fig. 12-A and confirmed by the EDS line scan in Fig. 13. No Mo-banding was visible in the fuel plate with heat treatment (Irr-C) after irradiation as

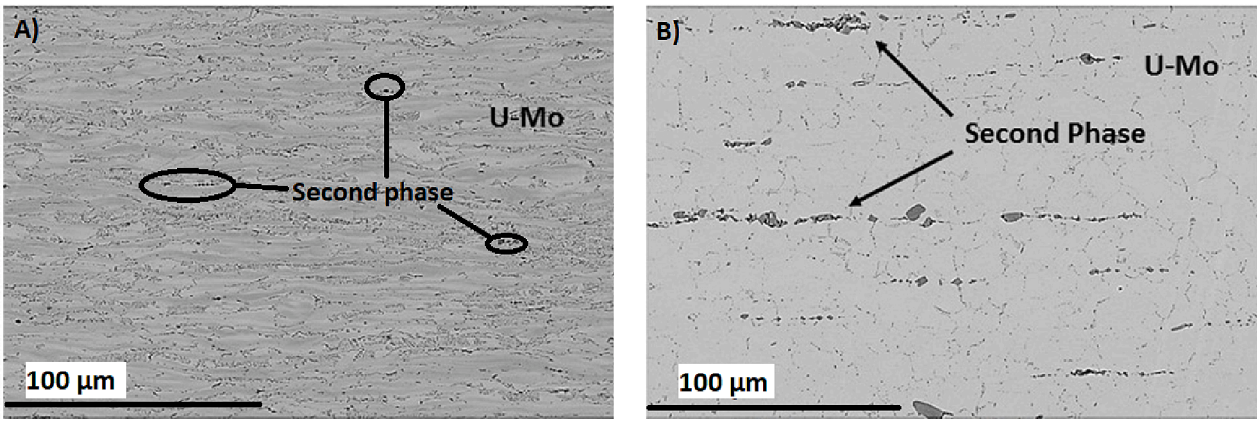

Fig. 9. Example of carbides and oxides precipitates, also called second phase, are shown for both unirradiated samples A) Unirr-B, and B)Unirr-C from Refs. [28].

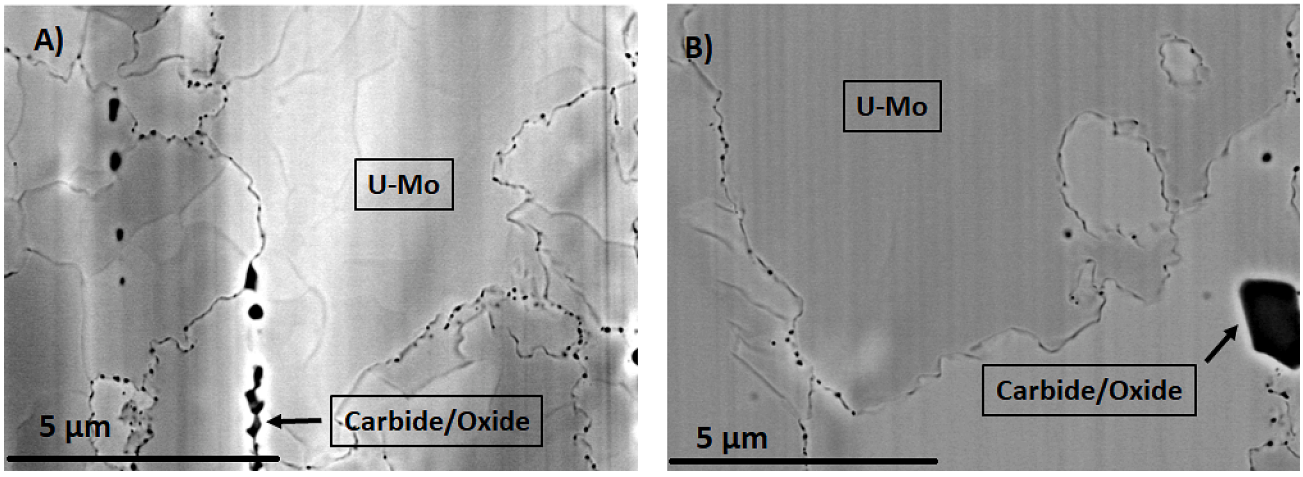

Fig. 10. Example of carbide and oxide precipitates after irradiation, A) sample Irr-B, B) sample Irr-C.

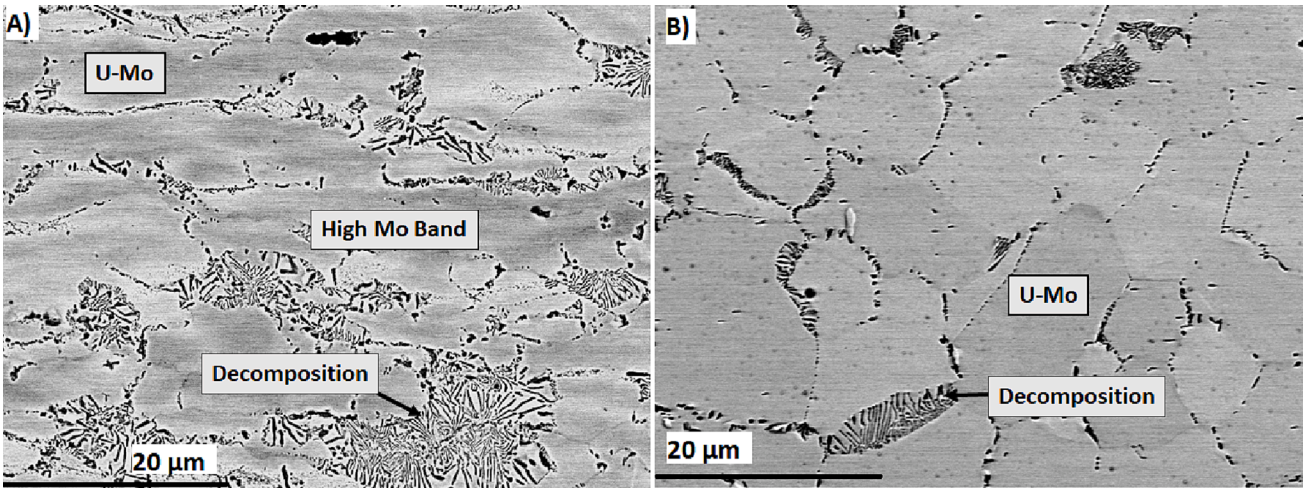

Fig. 11. SEM images showing microstructure and chemical variation in the samples before irradiation. A) Unirr-B shows chemical banding. B) Unirr-C shows homogenous composition and minimal decomposition.

expected and seen in Fig. 12-B.

Discussion

The analyzed samples show very different behavior after irradiation based on the fabrication method. The non-heat-treated samples present bands containing large amounts of decomposed gamma phase areas (namely α-U + U_2Mo) before irradiation. After irradiation, large clusters of micron-sized grains were observed in these areas. These grains are presumed to be in γ-U phase, which formed by an irradiation induced

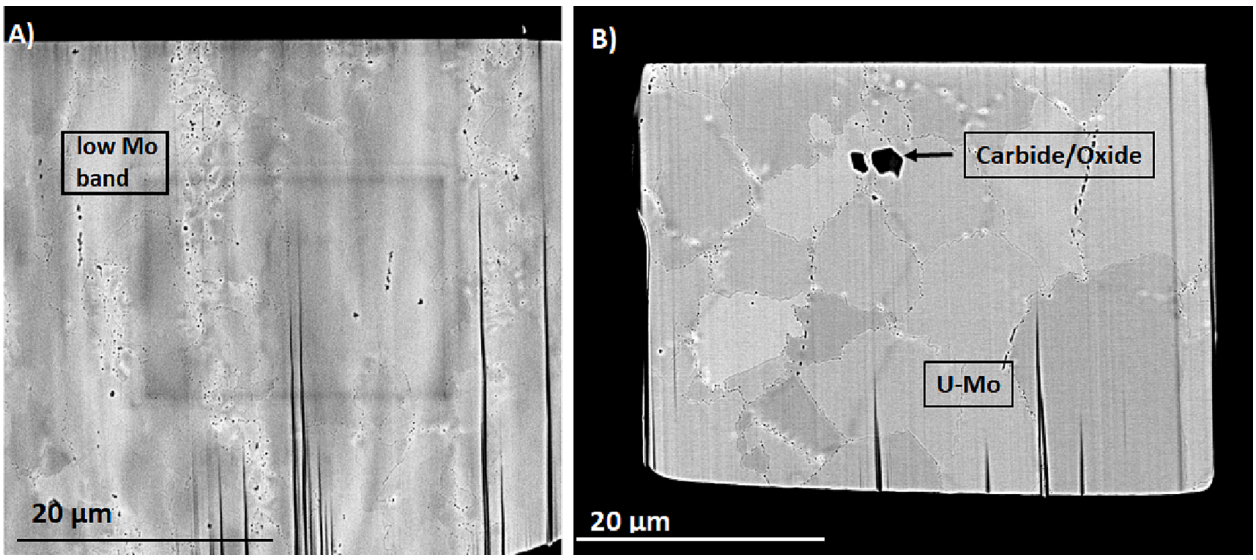

Fig. 12. SEM BSE images show that Irr-B in image A) maintains Mo banding after irradiation. While Irr-C (image B) shows homogeneous composition in the fuel core.

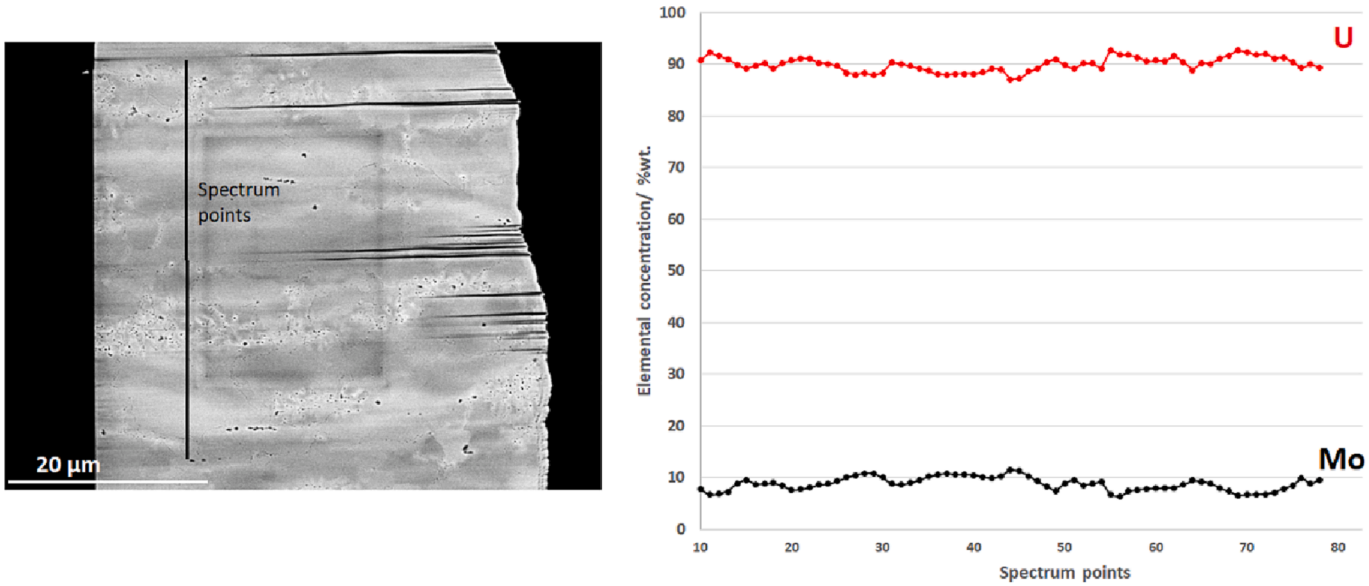

Fig. 13. EDS point line scan showing the variation in Mo concentration in the Irr-B sample.

reverse transformation in the early stage of irradiation (α-U + U_2Mo → γ-U), as shown in Fig. 14 and reported previously in reference [1]. This region may affect fuel performance. Indeed, grain boundaries are known to be the starting point of fission products precipitation (including gases and solid products) and thus of bubble formation from fission gases precipitation. Thus, the presence of larger amounts of grain boundaries in these regions could enhance swelling rates when compared to plates without these features, such as those that have been heat treated. This is in line with the results of previous studies showing that tailoring the initial microstructure of the fuel influences fission-induced recrystallization [6,7], can control fission gas diffusivity [7,8], and that controlling γ-phase decomposition can permit stable irradiation behavior of the fuel [1,12,17,30].

Moreover, after irradiation changes in grain boundaries characteristics were observed in both samples, with straight grain boundaries becoming wavy. A possible reason could be related to the incipit of grain refining process. Another reason could be the reverse γ-U transformation upon irradiation, described previously, that could also contribute to the wavy shape of the grain boundaries. As grain refining was observed near the U-Mo/Zr interface (mostly inside or near the low Mo sublayer) as shown in Fig. 15, this could confirm the relation of this phenomenon to the presence of α-U.

In previous work, porosities were observed to develop at the carbide and U-Mo interface [30], as mentioned this could be related to an increased α-U presence near these features. This was not observed at low burn-up and thus may start only later at higher burn-up as observed in ref.30.

The Zr layer shows similar features as observed in ref. [28] and was not affected in these early irradiation stages. A thicker UZr_2 layer was observed in the heat-treated sample before irradiation, similar to ref. [18]. This could enhance U-Mo and Zr bonding and thus, mechanical stability of the plate after irradiation. However, the porosity found in the low Mo sublayer near the U-Mo and Zr interface after irradiation at low burn-up, may influence swelling and blistering in this layer at higher burn-up. As observed in ref. [20,32] these fission gases porosities may grow and interconnect creating fission gases channel parallel to the

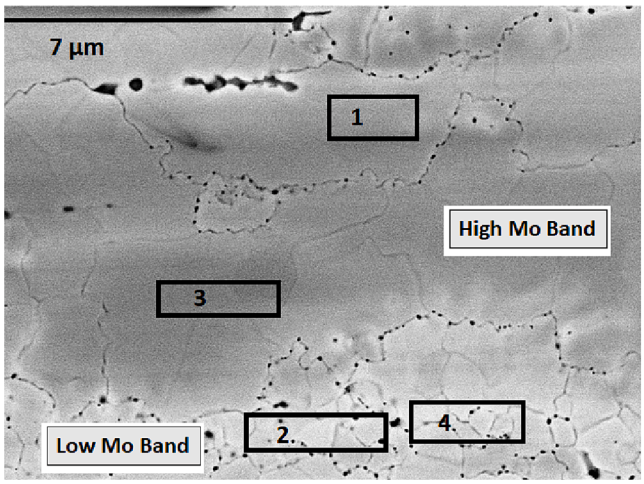

Spectrum	Composition %wt.	
	Mo	U
1	11.16	87.25
2	6.38	92.53
3	10.39	87.89
4	6.48	91.95

Fig. 14. Irradiated sample (Irr-B) showing reverse transformation with the presence of small grains in the low Mo band region. Minor elements (Nd, Xe, etc.) were not included in the table, thus the sum of the two elements of interest does not come to 100.

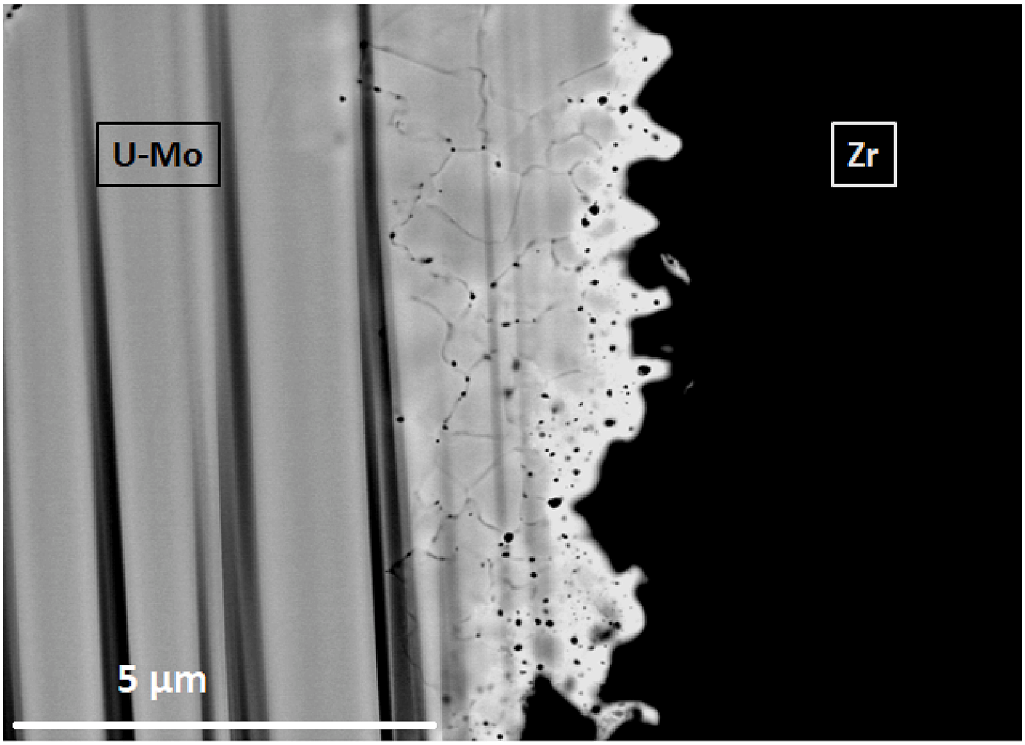

Fig. 15. Example of micron size grains near U-Mo/Zr interface.

interface and following generate enlarged porosities containing gases (e.g. blisters) which lead to cracks and fuel cladding failure. Thus, this phenomenon needs further characterization at higher burn-up to understand if the thicker U-Mo and Zr interaction layer can impact the interfacial porosity and precipitate size and interconnection and thus blistering.

Conclusions and summary

In this study we compared the irradiation behavior of U-Mo fuel foils produced with or without heat treatment. This process has been shown to influence the irradiation behavior even at low burn-up. Larger starting grain size was observed in the heat-treated samples. This generated less grain boundaries and led to decreased grain refining after irradiation. Associated to the presence of these small grains (grain refinement) nano-size bubbles and precipitates were found that could potentially influence fuel swelling performance. Large grains have been observed to slow down the formation of the porosity during the early stage of irradiation investigated in this study. Thus, the heat-treated sample may present favorable features for irradiation performance.

Moreover, when γ-U decomposition is present, typically associated with chemical banding or at grain boundaries, the decomposition disappeared after irradiation even at low burnup (less than 1×10^{21} fission/cm^3). This phenomenon is strong evidence of reverse transformation under irradiation. However, during this phase reversion, smaller grains (1–2 µm after irradiation vs 5–8 µm before irradiation) are formed in the previously decomposed region. Indeed, this phenomenon differs in the two samples as in the samples where minimal γ-U

decomposition was present (heat treated samples) also the grain size was less affected by this phenomenon. The presence of more grain boundaries may also influence the fuel performance, as these are regions where fission gases accumulate and can thus influence the swelling mechanism. Moreover, the minor Mo variation in the heat-treated samples, which will incur in less phase change (reverse transformation) could also enhance the consistency of the fuel behavior under irradiation. This may again indicate the importance of heat treating the fuel prior to irradiation.

The relation of the carbide and U-Mo interface with fission gases porosities and precipitates was not observed in this study at these low burn-ups and thus may start only later at higher burnups as observed in previous work. However, these second phases have been hypothesized to only have limited effect on the swelling of the fuel core.

Finally, the Zr layer was not influenced by the irradiation. However, the U-Mo and Zr interaction layer seem to be thicker in the heat-treated sample, as a thicker UZr_2 layer was observed. The influence on fuel performance of this thicker layer needs further evaluation, as it may enhance the mechanical stability of the plate or be a region prone to swelling and blistering.

Further analyses are necessary, at higher burn-up, to assess the exact impact on irradiation behavior of different texture, cold work in U-Mo, and how heat treatment can improve irradiation fuel performance. Moreover, this study may require a larger number of samples to be investigated to confirm these early observations.

CRediT authorship contribution statement

F.G. Di Lemma: Conceptualization, Data curation, Formal analysis, Investigation, Visualization, Writing – original draft, Writing – review & editing, Project administration. **J.F. Jue:** Conceptualization, Investigation, Writing – original draft, Writing – review & editing, Project administration, Supervision, Data curation, Formal analysis, Supervision. **T.L. Trowbridge:** Data curation, Formal analysis, Investigation, Visualization, Writing – review & editing, Project administration. **C.A. Smith:** Data curation, Formal analysis, Investigation, Visualization, Writing – review & editing, Project administration. **B.D. Miller:** Data curation, Formal analysis, Investigation, Project administration, Supervision, Writing – review & editing. **D.D. Keiser:** Conceptualization, Funding acquisition, Project administration, Writing – review & editing, Supervision. **J.J. Giglio:** Conceptualization, Funding acquisition, Project administration, Writing – review & editing, Supervision. **J.I. Cole:** Conceptualization, Funding acquisition, Project administration, Writing – review & editing, Supervision.

Declaration of Competing Interest

The authors declare that they have no known competing financial interests or personal relationships that could have appeared to influence the work reported in this paper.

Data availability

The authors do not have permission to share data.

Acknowledgments

The funding for this study was provided by the United States High-Performance Research Reactor Project, Office of Material Management and Minimization, National Nuclear Security Administration, from the U.S. Department of Energy under DOE-NE Idaho Operations Office Contract DE-AC07-05ID14517. The authors would like to acknowledge the staff of the Electron Microscopy Laboratory, of the Fuel and Applied Science Building, and of the Irradiated Material Characterization Laboratory at the Materials and Fuels Complex at Idaho National Laboratory for their effort in handling, preparing, and transferring of the specimens used in this work.

References

[1] M.K. Meyer, J. Gan, J.F. Jue, D.D. Keiser, E. Perez, A. Robinson, D.M. Wachs, N. Woolstenhulme, G.L. Hofman, Y.S. Kim, Irradiation performance of U-Mo Monolithic fuel, Nucl. Eng. Technol. 46 (2) (2014) 169–182, https://doi.org/10.5516/NET.07.2014.706.

[2] J.L. Snelgrove, G.L. Hofman, M.K. Meyer, C.L. Trybus, T.C. Weincek, Development of Very-High Density Low Enriched Uranium Fuels, Nucl. Eng. Des. 178 (1997) 119–126, https://doi.org/10.1016/S0029-5493(97)00217-3.

[3] J. Roglans-Ribas, C. Landers, Research and test reactor conversion to low enriched uranium fuel: technical and programmatic progress. International Conference on Research Reactors: Safe Management and Effective Utilization, Rabat, November, 2011.

[4] F.G. Di Lemma, J. Burns, J.W. Madden, A.J. Winston, A.B. Robinson, J.F. Jue, D. D. Keiser, J.I. Cole, Texture analyses and microstructural evolution in monolithic U-Mo nuclear fuel, J. Nucl. Mater. 544 (2021), 152677, https://doi.org/10.1016/j.jnucmat.2020.152677.

[5] O. Engler and V. Randle, Introduction to texture analysis: macrotexture, microtexture, and orientation mapping, 2nd edition, (2010), ISBN 978-1-4200-6365-3.

[6] S. Hu, D. Burkes, C.A. Lavender, V. Joshi, Effect of grain morphology on gas bubble swelling in UMo fuels – A 3D microstructure dependent Booth model, J. Nucl. Mater. 480 (2016) (2016) 323–331, https://doi.org/10.1016/j.jnucmat.2016.08.038.

[7] L. Liang, Z.G. Mei, Y.S. Kim, B. Ye, G. Hofman, M. Anitescu, A.M. Yacout, Mesoscale model for fission-induced recrystallization in U-7Mo alloy, Comp. Mater. Sci. 124 (2016) 228–237, https://doi.org/10.1016/j.commatsci.2016.07.033.

[8] L. Liang, Z.G. Mei, A.M. Yacout, Fission-induced recrystallization effect on intergranular bubble-driven swelling in U-Mo fuel, Comp. Mater. Sci. 138 (2017) 16–26, https://doi.org/10.1016/j.commatsci.2017.06.013.

[9] D.D. Keiser, J.F. Jue, N.E. Woolstenhulme, A. Ewh, Potential annealing treatments for tailoring the starting microstructure of low-enriched U-Mo dispersion fuels to optimize performance during irradiation, J. Nucl. Mater. 419 (1–3) (2011) 226–234, https://doi.org/10.1016/j.jnucmat.2011.08.039.

[10] T.A. Pedrosa, A.M. Matildes dos Santos, F.S. Lameiras, P.R. Cetlin, W.B. Ferraz, Phase transitions during artificial ageing of segregated as-cast U-Mo alloys, J. Nucl. Mater. 457 (2015) 100–117, https://doi.org/10.1016/j.jnucmat.2014.11.004.

[11] S. Jana, L. Sweet, D. Neal, A. Schemer-Kohrn, C. Lavender, V. Joshi, The role of ternary alloying elements in eutectoid transformation of U10Mo alloy part I. Microstructure evolution during arc melting and subsequent homogenization annealing in U9.8Mo0.2X alloy (X = Cr, Ni, Co), J. Nucl. Mater. 509 (2018) 318–329, https://doi.org/10.1016/j.jnucmat.2018.06.024.

[12] R. Newell, A. Mehta, D.D. Keiser, Y. Sohn, Phase reversion kinetics of thermally decomposed ($\alpha + \gamma'$) phases to γ-phase in U–10 wt% Mo alloy, J. Nucl. Mater. 530 (2020), 151983, https://doi.org/10.1016/j.jnucmat.2019.151983.

[13] T. Ajantiwalay, C. Smith, D.D. Keiser, A. Aitkaliyeva, A critical review of the microstructure of U-Mo fuels, J. Nucl. Mater. 540 (2020), 152386, https://doi.org/10.1016/j.jnucmat.2020.152386.

[14] A. Devaraj, E. Kautz, L. Kovarik, S. Jana, N. Overman, C. Lavender, V.V. Joshi, Phase transformation of metastable discontinuous precipitation products to equilibrium phases in U10Mo alloys, Scripta Mater. 156 (2018) 70–74, https://doi.org/10.1016/j.scriptamat.2018.07.010.

[15] W.E. Frazier, S. Hu, N. Overman, R. Prabhakaran, C. Lavender, V.V. Joshi, Recrystallization kinetics of cold-rolled U-10 wt% Mo, J. Nucl. Mater. 513 (2019) 56–61, https://doi.org/10.1016/j.jnucmat.2018.10.046.

[16] B.J. Schuessler, D.P. Field, N.R. Overman, V.V. Joshi, The Effect of Homogenization Heat Treatment on the Texture Evolution in U-10Mo Alloy, Metall. Mater. Trans A. 52 (2021) 3871–3879, https://doi.org/10.1007/s11661-021-06349-8.

[17] A.J. Clarke, K.D. Clarke, R.J. McCabe, C.T. Necker, P.A. Papin, R.D. Field, A. M. Kelly, T.J. Tucker, R.T. Forsyth, P.O. Dickerson, J.C. Foley, H. Swenson, R. M. Aikin, D.E. Dombrowski, Microstructural evolution of a uranium-10 wt.% molybdenum alloy for nuclear reactor fuels, J. Nucl. Mater. 465 (2015) 784–792, https://doi.org/10.1016/j.jnucmat.2015.07.004.

[18] F.G. Di Lemma, J.F. Jue, A.J. Winston, X. Pu, S. Anderson, D.D. Keiser, J.J. Giglio, J.I. Cole, Impacts of annealing treatment on the microstructure of U-Mo monolithic fuel plates, J. Nucl. Mater. 564 (2022), 153687, https://doi.org/10.1016/j.jnucmat.2022.153687.

[19] F. Rice, W. Williams, A. Robinson, J. Harp, M. Meyer, B. Rabin, RERTR-12 Post-irradiation Examination Summary Report, Technical Report Idaho National Laboratory, United States, 2015, https://doi.org/10.2172/1173078.

[20] J.F. Jue, D.D. Keiser, B.D. Miller, J.W. Madden, A.B. Robinson, B.H. Rabin, Effects of irradiation on the interface between U-Mo and zirconium diffusion barrier, J. Nucl. Mater. 499 (2018) 567–581, https://doi.org/10.1016/j.jnucmat.2017.10.072.

[21] J.F. Jue, D.D. Keiser, C.R. Breckenridge, G.A. Moore, M.K. Meyer, Microstructural characteristics of HIP-bonded monolithic nuclear fuels with a diffusion barrier, J. Nucl. Mater. 448 (1–3) (2014) 250–258, https://doi.org/10.1016/j.jnucmat.2014.02.004.

[22] J.F. Jue, T.L. Trowbridge, C.R. Breckenridge, G.A. Moore, M.K. Meyer, D.D. Keiser, Effects of heat treatment on U-Mo fuel foils with a zirconium diffusion barrier, J. Nucl. Mater. 460 (2015) 153–159, https://doi.org/10.1016/j.jnucmat.2015.02.017.

[23] D. Jadernas, J. Gan, D. Keiser, J. Madden, M. Bachhav, J.F. Jue, A. Robinson, Microstructural characterization of as-fabricated and irradiated U-Mo fuel using SEM/EBSD, J. Nucl. Mater. 509 (2018) 1–8, https://doi.org/10.1016/j.jnucmat.2018.06.007. ISSN 0022-3115.
[24] A. Aitkaliyeva, J.W. Madden, B.D. Miller, J.I. Cole, Implementation of focused ion beam (FIB) system in characterization of nuclear fuels and materials, Micron 67 (2014) 65–73, https://doi.org/10.1016/j.micron.2014.06.010.
[25] C. Li, G. Habler, L.C. Baldwin, R. Abart, Ultramicroscopy An improved FIB sample preparation technique for site-specific plan-view specimens : A new cutting geometry, Ultramicroscopy. 184 (2018) 310–317, https://doi.org/10.1016/j.ultramic.2017.09.011.
[26] D. Salvato, A. Leenaers, S. Van den Berghe, C. Detavernier, Pore pressure estimation in irradiated U-Mo, J. Nucl. Mater. 510 (2018) 472–483, https://doi.org/10.1016/j.jnucmat.2018.08.039.
[27] A. Leenaers, W. Van Renterghem, S. Van den Berghe, High burn-up structure of U (Mo) dispersion fuel, J. Nucl. Mater 476 (2016) 218–230, https://doi.org/10.1016/j.jnucmat.2016.04.035.
[28] J.F. Jue, D.D. Keiser Jr, J.W. Madden, B.D. Miller "Characterization of the Zr diffusion barrier in base monolithic U-10Mo fuel" Technical Report Idaho National Laboratory, INL/LTD-16-39665, (2016).
[29] J.F. Jue, D.D. Keiser Jr, J.W. Madden, A.B. Robinson, T. Trowbridge, "The Impact of Impurities in U–Mo" Technical Report Idaho National Laboratory, INL/LTD-19-54046, (2019).
[30] C. Smith, J.F. Jue, T. Trowbridge, D. Keiser, J. Madden, A. Robinson, J. Giglio, Possible impacts of Mo chemical banding and second phase impurities on the irradiation behavior of monolithic U-10Mo fuels, J. Nucl. Mater 576 (2023), 154264, https://doi.org/10.1016/j.jnucmat.2023.154264.
[31] D.E. Burkes, R. Prabhakaran, T. Hartmann, J.F. Jue, F.J. Rice, Properties of Du-10wt% Mo alloys subjected to various post rolling heat treatments, J. Nucl. Eng. Des. 240 (6) (2010) 1332–1339, https://doi.org/10.1016/j.nucengdes.2010.02.008.
[32] C. Smith, J.F. Jue, D. Keiser, T. Trowbridge, B. Miller, A. Robinson, A. Winston, J. Giglio, An investigation of the failure modes in U-10Mo monolithic fuel irradiated to high burnup, J. Nucl. Mater 575 (2023), 154202, https://doi.org/10.1016/j.jnucmat.2022.154202.